Identification of a distal enhancer regulating hedgehog interacting protein gene in human lung epithelial cells

Feng Guo,[a,b,m,*] Li Zhang,[a,c,m] Yuzhen Yu,[a] Lu Gong,[a] Shiyue Tao,[d] Rhiannon B. Werder,[e,f] Shreya Mishra,[h] Yihan Zhou,[a] Wardatul Jannat Anamika,[a] Taotao Lao,[a] Hiroyuki Inuzuka,[g] Yihan Zhang,[i] Betty Pham,[a] Tao Liu,[a] Tiffany S. Tufenkjian,[j,k] Bradley W. Richmond,[j,k] Wenyi Wei,[g] Hongmei Mou,[i] Andrew A. Wilson,[e,f] Ming Hu,[h] Wei Chen,[d,l] and Xiaobo Zhou[a,**]

[a]Channing Division of Network Medicine, Department of Medicine, Brigham and Women's Hospital and Harvard Medical School, Boston, MA 02115, USA
[b]Jiangsu Key Laboratory of Immunity and Metabolism, Department of Pathogenic Biology and Immunology, Xuzhou Medical University, Xuzhou, Jiangsu 221004, China
[c]Department of Integrated Traditional Chinese and Western Medicine, West China Hospital, Sichuan University, Chengdu, Sichuan 610041, China
[d]Department of Biostatistics, School of Public Health, University of Pittsburgh, Pittsburgh, PA 15224, USA
[e]Center for Regenerative Medicine of Boston University and Boston Medical Center, Boston, MA 02118, USA
[f]The Pulmonary Center and Department of Medicine, Boston University School of Medicine, Boston, MA 02118, USA
[g]Department of Pathology, Beth Israel Deaconess Medical Center, Harvard Medical School, Boston, MA 02115, USA
[h]Department of Quantitative Health Sciences, Lerner Research Institute, Cleveland Clinic Foundation, Cleveland, OH 44195, USA
[i]The Mucosal Immunology and Biology Research Center, Massachusetts General Hospital and Harvard Medical School, Boston, MA 02114, USA
[j]Department of Veterans Affairs Medical Center, Nashville, TN 37232, USA
[k]Division of Allergy, Pulmonary, and Critical Care Medicine, Department of Medicine, Vanderbilt University Medical Center, Nashville, TN 37232, USA
[l]Division of Pediatric Pulmonary Medicine, UPMC Children's Hospital of Pittsburgh, University of Pittsburgh, Pittsburgh, PA 15224, USA

eBioMedicine
2024;101: 105026
Published Online 27 February 2024
https://doi.org/10.1016/j.ebiom.2024.105026

Summary

Background An intergenic region at chromosome 4q31 is one of the most significant regions associated with COPD susceptibility and lung function in GWAS. In this region, the implicated causal gene *HHIP* has a unique epithelial expression pattern in adult human lungs, in contrast to dominant expression in fibroblasts in murine lungs. However, the mechanism underlying the species-dependent cell type-specific regulation of *HHIP* remains largely unknown.

Methods We employed snATAC-seq analysis to identify open chromatin regions within the COPD GWAS region in various human lung cell types. ChIP-quantitative PCR, reporter assays, chromatin conformation capture assays and Hi-C assays were conducted to characterize the regulatory element in this region. CRISPR/Cas9-editing was performed in BEAS-2B cells to generate single colonies with stable knockout of the regulatory element. RT-PCR and Western blot assays were used to evaluate expression of *HHIP* and epithelial–mesenchymal transition (EMT)-related marker genes.

Findings We identified a distal enhancer within the COPD 4q31 GWAS locus that regulates *HHIP* transcription at baseline and after TGFβ treatment in a SMAD3-dependent, but Hedgehog-independent manner in human bronchial epithelial cells. The distal enhancer also maintains chromatin topological domains near 4q31 locus and *HHIP* gene. Reduced *HHIP* expression led to increased EMT induced by TGFβ in human bronchial epithelial cells.

Interpretation A distal enhancer regulates *HHIP* expression both under homeostatic condition and upon TGFβ treatment in human bronchial epithelial cells. The interaction between HHIP and TGFβ signalling possibly contributes to COPD pathogenesis.

Funding Supported by NIH grants R01HL127200, R01HL148667 and R01HL162783 (to X. Z).

*Corresponding author. 221 Longwood Ave, EBRC 620C, Boston, MA 02115, USA.
**Corresponding author. 221 Longwood Ave, EBRC 620C, Boston, MA 02115, USA.
E-mail addresses: Feng.Guo@xzhmu.edu.cn (F. Guo), Xiaobo.Zhou@channing.harvard.edu (X. Zhou).
[m]Authors contributed equally.

Keywords: Chronic obstructive pulmonary disease; Distal enhancer; Hi-C; Epithelial-mesenchymal transition; TGFβ; Epigenetics

Research in context

Evidence before this study

The strongest and most replicated genetic association signals in chronic obstructive pulmonary disease (COPD) through genome-wide association studies (GWAS) reside in an intergenic region at 4q31, near the Hedgehog Interacting Protein (*HHIP*) gene. We have previously linked the intergenic association signals to the causal gene, *HHIP*, and also demonstrated increased emphysema in *Hhip* haploinsufficient mice after either 6 months of chronic cigarette smoke exposure or ageing. However, relatively little is known about the transcriptional regulation of *HHIP* by this GWAS region, especially in human lung epithelial cells, a major cell type that expresses HHIP in human adult lungs. Our study aims to determine the mechanism of epithelial expression of HHIP, and how such regulation responds to COPD-relevant stimulations such as TGFβ treatment. In summary, our previous work successfully linked the 4q31 intergenic GWAS locus in COPD with *HHIP*. Herein, we extended our previous research to identify a human unique distal enhancer at the 4q31 GWAS locus that regulates the expression of HHIP in human lung epithelial cells. Furthermore, whether and how this enhancer responds to TGFβ treatment is also evaluated.

Added value of this study

1) We identified a distal enhancer for *HHIP*.
2) The distal enhancer maintains local chromatin structure.
3) TGFβ induces the expression of HHIP in human lung epithelial cells.

Implications of all the available evidence

COPD is the third leading cause of mortality worldwide, without a cure yet. *HHIP* is one of the most replicated genes associated with COPD GWAS study. We identified a distal enhancer located in the 4q31 COPD GWAS locus, which regulates *HHIP* expression in human bronchial epithelial cells. Depletion of the distal enhancer led to a profound loss of chromatin interaction near *HHIP* gene. Our work revealed chromatin 3D structure in BEAS-2B cells, and identified the regulation of *HHIP* gene by the distal enhancer and by TGFβ, known to be involved in COPD pathogenesis.

Introduction

Hedgehog interacting protein (*HHIP*) is one of the most replicable genes identified by genome-wide association studies (GWAS) implicated in chronic obstructive pulmonary disease (COPD), the third leading cause of global death.[1–4] The GWAS locus at 4q31 near *HHIP* in COPD is also shared by GWAS of lung function in the general population, suggesting the importance of HHIP in maintaining lung homeostasis and/or lung development given its inhibitory roles in the Hedgehog pathway by competitive binding with three Hedgehog ligands.[5] Indeed, HHIP is required for normal lung development as *Hhip* knockout mice died immediately after birth due to significantly reduced lung size and lung branching defects caused by hyperactivation of the Hedgehog pathway.[6]

In addition to its critical role in lung development, HHIP is also important for COPD pathogenesis. As we reported previously, *Hhip* haploinsufficient ($Hhip^{+/-}$) mice showed increased susceptibility to smoke-induced or age-related emphysema,[7,8] associated with increased oxidative stress after cigarette smoke exposure and/or increased lymphocyte activation in murine lungs during ageing,[7–9] recapitulating human COPD development in subjects carrying risk alleles. However, the transcriptional regulation of *HHIP* under both homeostatic and pathological conditions, which are relevant to COPD development, remains largely elusive. This is particularly significant given our ongoing efforts to translate human GWAS findings into a better understanding of COPD pathogenesis, as well as to design treatment strategies. Under homeostatic condition, recent single-cell RNA sequencing (scRNA-seq) data revealed expression pattern of HHIP in distinct epithelial cells in adult human lungs, suggesting a unique transcriptional regulation mechanism for *HHIP* in human lung epithelial cells.

Transforming growth factor β (TGFβ) is an important pleiotropic factor that regulates a myriad of biological processes, including development, tissue regeneration, immune responses and tumorigenesis.[10–12] Additionally, TGFβ-induced epithelial–mesenchymal transition (EMT)[13,14] also contributes to airway remodelling, a common pathological condition seen in COPD[15–17] and $Hhip^{+/-}$ mice after chronic cigarette smoke exposure.[18] Therefore, it is imperative to determine the possible crosstalk between TGFβ and HHIP in lung-relevant cell type.

In our study, by assessing chromatin interaction and histone enrichment in human lung epithelial cells, we

identified a distal enhancer at 4q31 regulating the expression of *HHIP* through forming chromatin loops at the basal level and also responding to the induction of TGFβ. Depletion of *HHIP* induced more significant EMT under TGFβ1 treatment in human bronchial epithelial cells.

Methods

Ethics

Human lung samples were collected under a protocol approved by the Institutional Review Board of Vanderbilt University Medical Center (IRB#060165). All participants provided informed consent.

snATAC plus snRNA-seq COPD lung tissue

Human COPD distal lung tissues were collected from patients (n = 3) who underwent lung transplantation for advanced COPD at Vanderbilt University Medical Center (IRB #060165). Fresh tissue was collected shortly after transplant and then minced and cryopreserved in 90% FBS and 10% DMSO. On the day of sequencing, thawed tissue was digested in an enzymatic cocktail (Miltenyi Multi-Tissue Dissociation Kit 1) using a gentleMACS Octo Dissociator (Miltenyi, Inc). Digested lung samples were serially filtered through 100 μm, and 40 μm cell strainers and treated with DNase1. Red blood cells were lysed using ACK buffer. Cell suspensions then underwent magnetic bead-based sorting for EPCAM + cells (Miltenyi Microbeads) followed by nuclei isolation. For COPD-62 and COPD-63, snap-frozen lung tissues were ground and processed for nuclei isolation using a Chromium nuclei isolation kit with RNase inhibitor (10× Genomics). Nuclei samples from COPD lungs were processed using the Chromium Next GEM Single Cell Multiome ATAC + Gene Expression reagent kit according to the manufacturer's instructions. Sequencing (Single Cell Multiome ATAC + Gene expression, v1 chemistry) was performed in the Vanderbilt Technologies for Advanced Genomics (VANTAGE) Core or Admera Health using a NovaSeq 6000 (Illumina) targeting 20,000 reads/cell for gene expression libraries and 25,000 reads/cell for ATAC-Seq libraries. The clinical characteristics of COPD subjects are listed in Supplementary Table S1. Sex of patients with COPD was determined by biological secondary sex characteristics.

Single-nucleus multiome data analysis

Our analysis was processed with the Seurat (version 4.4.0) and Signac (version 1.9.0) packages in R.[19,20] Cells with ATAC counts either above 20,000 or below 100, and RNA counts either above 10,000 or below 100 were filtered out. Additional parameters for cell quality included nucleosome signal below 2 and TSS enrichment above 1. Peak calling was executed by MACS2 (Model-based Analysis for ChIP-Seq) to discern peaks from aggregated fragment data.[21] We finally include 36,601 genes and 35,896 peaks across 12,015 cells in our forward analysis.

We utilised Azimuth to perform the cell type annotation,[19] referencing the gene expression dataset consists of 65,662 human lung cells from Travaglini et al., 2020.[22] We organised cell types into groups aligned with their functional characteristics and lineage, including 'myeloid progenitor cell'—comprising macrophages, CD14+ monocytes, CD16+ monocytes, dendritic cells, and plasmacytoid dendritic cells; and 'lymphoid progenitor cell'—encompassing CD4+ T cells, CD8+ T cells, B cells, and natural killer cells. Endothelial cells were assorted into subgroups such as lymphatic, capillary (including aerocyte and intermediate types), artery, and vein, each reflective of their unique vascular roles. Similarly, mesenchymal cells, including fibroblasts, myofibroblasts, mesothelial cells, and pericytes, were categorised based on their distinct functionalities within lung tissue. The cell types with fewer than 50 cells were excluded from our study.

Cell culture

Human BEAS-2B bronchial epithelial cells were purchased from ATCC and cultured with SAGM BulletKit (Lonza, CC-3118). Primary normal human bronchial epithelial (NHBE) cells were purchased from ATCC (PCS-300-010) and Lonza (CC-2540) and cultured with the BEGM BulletKit (Lonza, CC-3170). The air-liquid interface (ALI) differentiation was performed as we described previously.[23]

siRNA transfection

For siRNA transfection, BEAS-2B cells were transfected with *SMAD2* (L-003561-00-0005), *SMAD3* (L-020067-00-0005), or non-targeting siRNA pool (D-001810-10-05) separately at 60% confluency using Lipofectamine RNAiMAX (Thermo Fisher, 13778150) in 6-well plates. All siRNA pools were purchased from Dharmacon. Knockdown efficiency was confirmed by RT-PCR 48 h post-transfection.

Western blotting

Total protein samples were extracted from cell samples by 2× laemmli sample buffer (Bio-Rad, 1610737), separated by SDS-PAGE and transferred to a PVDF membrane. Primary antibodies include anti-N-Cadherin (4061S), anti-Slug (9585S), anti-Snail (3879S), anti-phospho-SMAD2 (3108S), anti-SMAD2 (3103S), anti-phospho-SMAD3 (9520S) from Cell Signalling Technology, and anti-SMAD3 (ab28379), anti-β-actin HRP (ab49900) from Abcam. HHIP primary antibody is from Santa Cruz (SC-293265), and Vinculin primary antibody is purchased from Sigma–Aldrich (V4505). Proteins were detected using ECL substrate (Pierce) and images were captured in the G:Box system (Syngene) as we have done previously.[24]

Chromatin immunoprecipitation (ChIP) assay

ChIP assays were carried out from cross-linked BEAS-2B cells with or without TGFβ1 treatment. Briefly, cells were cross-linked in 1% formaldehyde for 10 min, then glycine was added to quench the formaldehyde at a final concentration of 125 mM. After cell lysis and sonication, cell lysate was incubated overnight with various antibodies: anti-H3K27Ac (Abcam, ab4729), anti-SMAD3 (Abcam, ab28379) or rabbit isotype control IgG (Santa Cruz Biotechnology, sc-2027). Immunoprecipitated chromatin was then collected after incubation with protein A magnetic beads (Pierce, 88,845) at 4 °C for 4 h. After reverse cross-linking, DNA products were purified by MinElute PCR Purification Kit (QIAGEN, 28,006). The Quantitative real-time PCR (qPCR) was performed to identify the relative amount of ChIP products compared to the input by primers targeting human *HHIP* promoter and enhancer regions. Primer sequences used for ChIP-qPCR are listed in Supplementary Table S2.

Chromatin conformation capture assay (3C)

Briefly, 1×10^7 human BEAS-2B cells were cross-linked and lysed, and chromatin was digested with BglII (New England Biolabs, R0144S) at 37 °C overnight. Cross-linked and digested DNA fragments were ligated with T4 DNA ligase (New England Biolabs, M0202L) at 16 °C for 6 h 3C products were detected with 3C unidirectional PCR primers in triplicate PCR reactions as we have done previously.[25] Bacterial artificial chromosome (BAC) plasmids RP11-60L2 and RP11-767L24 were used for controls after going through the same protocol of digestion and ligation as the cellular templates. 3C-PCR primers were designed to target DNA fragments at sizes between 1 and 10 kb after BglII digestion. We also avoid primers designed for highly repeated genomic regions due to possible low specificity. Primer sequences used for 3C-PCR are listed in Supplementary Table S3.

Molecular cloning and reporter assays

HHIP enhancer regions at various lengths were cloned into the pGL3-Basic (Promega, E1751) vector amplified from BAC clones containing 670 bp of the *HHIP* promoter region (hg38, chr4:144,645,487–144,646,156) inserted by BglII and HindIII restriction enzyme. *HHIP* enhancer regions were cloned into the vector at the 5-end of *HHIP* promoter by BglII at either orientation, forward or reverse. All plasmids used for reporter assays were confirmed by Sanger sequencing. We performed reporter assays in BEAS-2B cells as previously described.[25] Briefly, 50% confluent BEAS-2B cells were seeded into a 48-well plate for transfection. Forty-eight hours after transfection with various reporter constructs along with TK-renilla, cell protein lysates were prepared for Dual-Glo Luciferase Reporter Assay System (Promega, E2920) according to the manufacturer's protocol. Luminescence signals were captured in a microplate reader (BioTek, Synergy H1). Firefly signals were normalised to TK-renilla signals, and then normalised to *HHIP* promoter-transfected cells to calculate enhancer activities for each construct. Primer sequences used for cloning reporter constructs are listed in Supplementary Table S4.

Conservation analysis

Conservation analysis between humans and mice (Fig. 2d and e) are displayed in green wiggle track according to the UCSC genome browser (human hg38). The Multiz Align view was selected to display the results.[26]

Generation of *HHIP* enhancer region knockout or *HHIP* knockout by CRISPR/Cas9

To generate *HHIP* enhancer region T2 knockout or HHIP knockout (*HHIP* KO) in BEAS-2B cells, guide RNAs were cloned into pSpCas9 (BB)-2A-Puro (PX459) V2.0 vector (Addgene, 62,988), separately. Plasmids with confirmed sequences were transfected into BEAS-2B cells with Lipofectamine 3000 (Thermo Fisher, L3000015) according to the manufacturer's instructions. Forty-eight hours after transfection, cells were selected with 1.0 μg/mL puromycin for 3 days. Then live cells were serially diluted and plated in 96-well plates to generate individual colonies that were subsequently expanded and verified by sequencing. Empty vector PX459-transfected cells were used as controls that went through exactly the same process of single colony selection with limited dilution followed by expansion. gRNA sequences used for enhancer or *HHIP* knockout are listed in Supplementary Table S5.

Generation of *HHIP* enhancer region knockout in iAT2

Ribonucleoprotein (RNP) complex with gRNA targeting the HHIP enhancer was performed by electroporation in induced pluripotent stem cell (iPSC)-derived alveolar type II epithelial cells (iAT2). Alt-R S.p. Cas9 Nuclease, crRNA and tracrRNA were ordered from IDT, and the manufacturer's instructions were followed for RNP complex assembly. iAT2 were differentiated, maintained, and electroporated with RNP complex as we described previously.[27] crRNA sequences are listed in Supplementary Table S6.

Hedgehog pathway agonist and antagonist treatment

Primary NHBE cells were starved and cultured with basic BEGM medium overnight followed by the treatment with TGFβ1 (R&D Systems, 7754-BH) (5 ng/mL), Hedgehog pathway agonist, SAG (Selleckchem, S6384) (50 nM), an agonist of Smoothened, or various Hedgehog pathway inhibitors, Vismodegib (Selleckchem, S1082) (10 μM), the Smoothened antagonist, Sonidegib (Selleckchem, S2151) (5 μM), and the GLI1 inhibitor,

GANT61 (Selleckchem, S8075) (10 μM) for 24 h separately or together as indicated in the figure legends.

Hi-C sample generation and sequencing data analysis

Clonal BEAS-2B cells (~2.5 million cells in each line) with either PX459 (Addgene, 62,988) vector control or T2 enhancer knockout were collected and crosslinked with 2% of formaldehyde (Fisher scientific, LC146501). Then the standard protocol of the Arima-HiC Kit was followed for the Hi-C sample generation according to the manufacturer's protocols (Arima Genomics, A510008). The samples were sequenced with Novaseq X plus a platform with 150bp read length, paired-end sequencing setting (Admera Health, NJ). The sequencing depth was 500 million reads per sample with two biological replicates for each clonal line.

We used Chromap[28] to map the paired end raw *fastq* files from Hi-C experiments to the reference genome hg38. We then removed PCR duplicates, and only kept uniquely mapped reads. Next, we applied the Juicer pipeline[29] to convert the mapped reads into *.hic* file and visualize them in the Juicebox.[30] Lastly, we used the KR-normed 50 Kb bin resolution Hi-C contact matrix for all the downstream analysis.[31]

The HUVEC Hi-C data (Fig. 3e) were obtained from the public database (GSE63525),[31] and visualised using Juicebox.

H3K27Ac ChIP-seq analysis

The results of the H3K27Ac ChIP-seq analysis from human lung tissues (Fig. 3a) are obtained from the public database with the following accession number and experiment number (16 years, ENCFF416LBI, ENCSR510RPC; 40 years, ENCFF314IJY, ENCSR494WCX; 60 years, ENCFF189JKC, ENCSR837DVF).[32] The results of the H3K27Ac ChIP-seq analysis from human new-born umbilical vein endothelial cell (HUVEC) cells (Fig. 3e) are obtained from the public database with the following accession number and experiment number (HUVEC, ENCFF089DEG, ENCSR000ALB).[32] Signal *P*-value files were chosen and visualised using Juicebox.

Cells, reagents and kits information

The detailed information of cells, reagents and kits are listed in Supplementary Table S7, including supplier name, catalogue numbers, and RRID tag.

Statistical analysis

All data were shown as mean ± SD. An unpaired *t*-test was used for a two-group comparison. Ordinary one-way ANOVA analysis followed by Dunnett comparisons was used for multi-group statistical analysis, and two-way ANOVA followed by Bonferroni comparisons were used for two variables comparison except special statements.

Role of funders

The funders had no role in study design, data collection, data analyses, interpretation, and decision to prepare or publish the manuscript.

Results

Enrichment of open chromatin at 4q31 COPD GWAS region in human lung epithelial cells

Under the homeostatic condition, *Hhip* is mainly expressed in mesenchymal cells in mouse lungs (Supplementary Fig. S1a and b) with an additional epithelial expression of *HHIP* in human lungs (Supplementary Fig. S1c and d), as shown by recent single-cell RNA sequencing (scRNA-seq) data.[22,33,34] To confirm this, we measured HHIP expression in human distal lung tissue and various primary human lung cells isolated from a healthy non-smoker donor as described before,[35] and BEAS-2B cells, an immortalised human bronchial epithelial line. Indeed, we detected higher *HHIP* mRNA levels in primary human alveolar type II epithelial cells (AT2), induced pluripotent stem cell (iPSC)-derived alveolar type II epithelial cells (iAT2) and BEAS-2B cells as compared to normal human lung fibroblasts (NHLF) (Supplementary Fig. S1e and f).

Since *HHIP* expression level is decreased in COPD lungs,[25] it is important to explore the possible mechanism of the transcriptional regulation of *HHIP* in human lung cells. Thus, we compared the epigenetic landscape revealed by single nucleus transposase-accessible chromatin using sequencing (ATAC-seq) in human lungs.[36] Within the 4q31 COPD GWAS region, a significant ATAC-Seq peak is detected in human lung epithelial cells from both healthy donors (Fig. 1a) and patients with COPD (Fig. 1b), suggesting the presence of a distal regulatory region, about 60 kb upstream of the *HHIP* gene promoter in the lungs from healthy donors (Fig. 1c) and from patients with COPD (Fig. 1d).

Identification of a human unique distal enhancer of *HHIP* gene at 4q31 locus

To investigate the regulatory element for *HHIP*, we initially assessed the enrichment of acetylation of lysine 27 of the H3 histone (H3K27Ac), a known marker for active enhancer or promoter. By performing Chromatin Immunoprecipitation (ChIP) followed by quantitative PCR (qPCR) in BEAS-2B cells, we detected H3K27Ac enrichment near the ATAC-Seq peak that was previously identified in human lung epithelial cells within the 4q31 GWAS region (Fig. 2a and b). Indeed, this region contains two enhancers: T2 (~1.1 kb) and T4 (~1.4 kb) for the endogenous *HHIP* promoter (~15–40 fold) in either forward or reverse orientation, as shown in reporter assay in BEAS-2B cells (Fig. 2c).

Given differential expression pattern of *HHIP* between mouse and human lungs, we also examined the

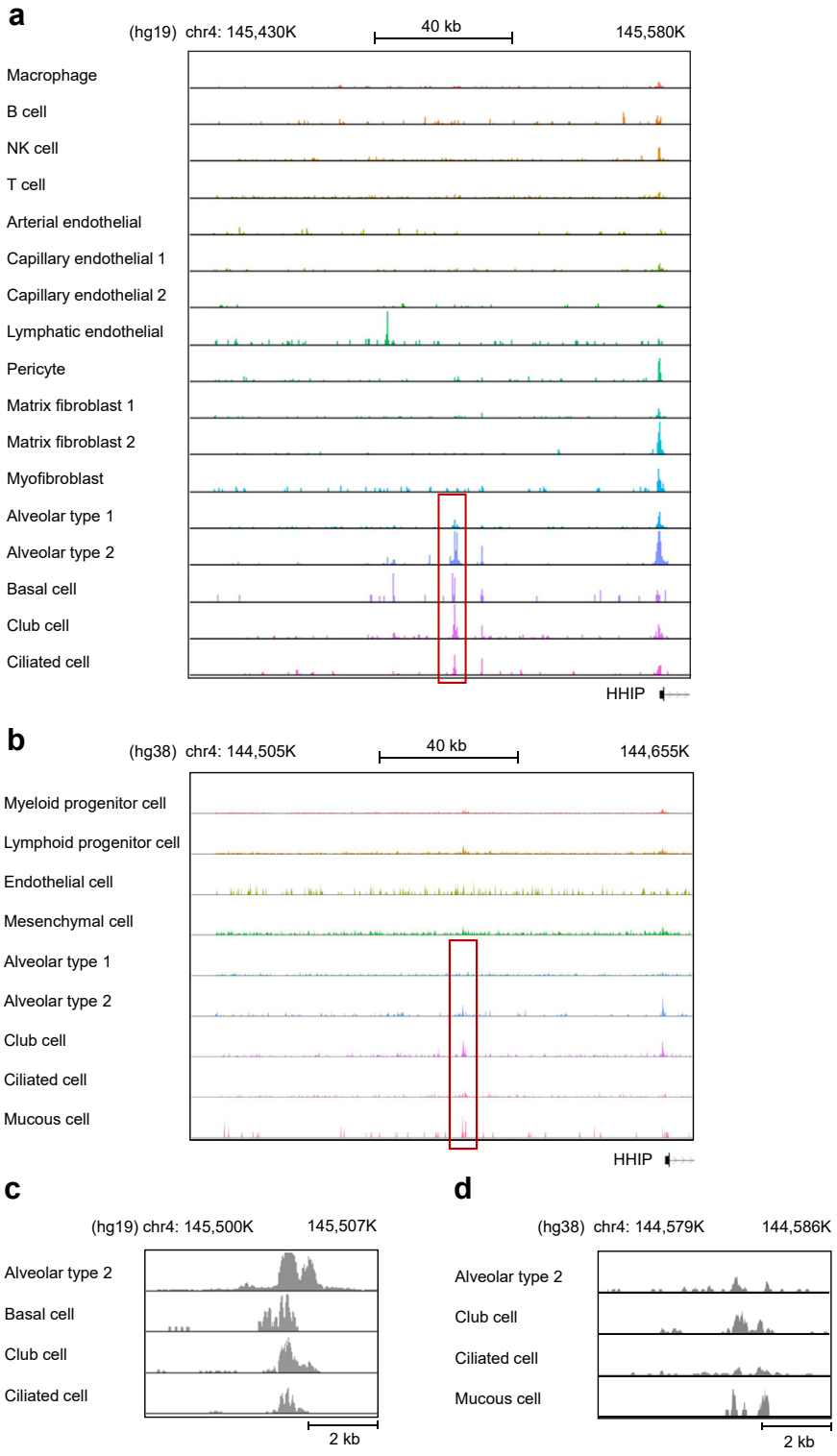

Fig. 1: **The open chromatin landscape upstream of *HHIP* in human lung cells.** (a) Single-cell ATAC-Seq peaks in healthy lungs from the public dataset (GSE 161383) (n = 3) and (b) single-nuclear ATAC-Seq peaks from patients with COPD (n = 3) within the 4q31 COPD GWAS locus across various cell types (Y axis scale range = 30). The highest peaks in the 4q31 region in human lung epithelial cells are indicated by the red frame. (c) Zoom-in view of the region in the red frame of (a) (chr4: 145,500K-145,507K, hg19) in epithelial cell types (Y = 40). (d) Zoom-in view of the region in the red frame from b (chr4: 144,579K-144,586K, hg38) in epithelial cell types (Y = 15).

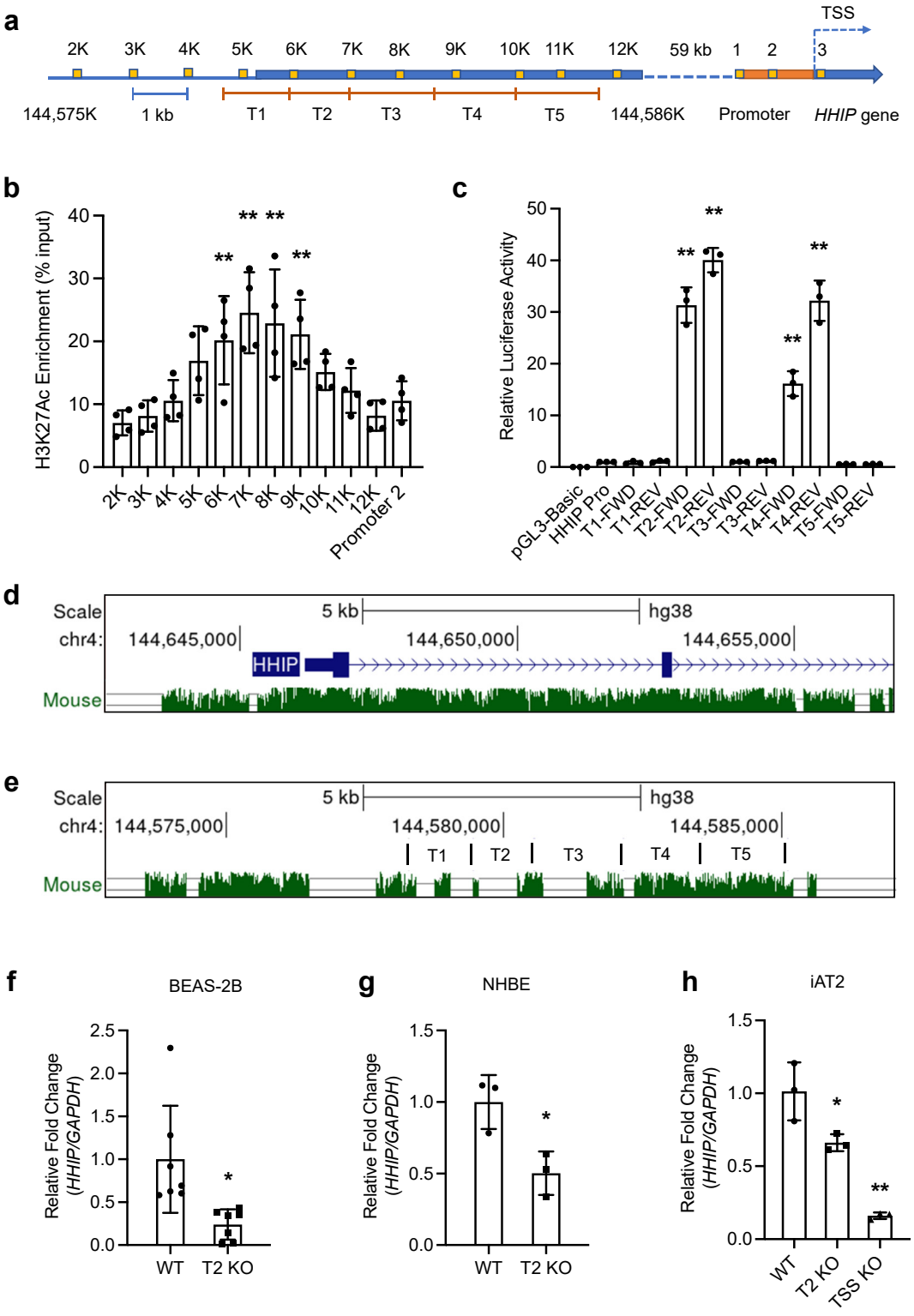

Fig. 2: **Identification of an *HHIP* distal enhancer in human lung epithelial cells.** (a) A schematic diagram shows the location of primers used to detect distal enhancers in chromatin immunoprecipitation (ChIP)-qPCR (b) and reporter assays (c). (b) H3K27Ac ChIP-qPCR results in BEAS-2B cells (n = 4 independent repeats) (Statistical analysis: ordinary one-way ANOVA analysis followed by Dunnett comparisons). (c) Reporter

conservation of the HHIP promoter and found it was highly conserved between human and mouse, especially around transcription start site (Fig. 2d). However, the novel T2 enhancer instead of the T4 enhancer at the 4q31 GWAS locus is poorly conserved between human and mouse genome (Fig. 2e), explaining the differential regulation mechanism between human and mouse *HHIP* possibly through the T2 human unique distal enhancer. We therefore focus on T2 enhancer for subsequent experiments.

Furthermore, knockout of endogenous T2 enhancer by gRNAs led to significantly decreased expression of *HHIP* in BEAS-2B cells (Fig. 2f) and normal human bronchial epithelial cells (NHBE) (Fig. 2g). Given abundant expression of *HHIP* in human AT2 cells (Supplementary Fig. S1e and f), we also generated knockout (KO) of T2 enhancer in iPSC-derived AT2 cells (iAT2 cells) by CRISPR/Cas9,[27] which led to reduced expression of *HHIP* (Fig. 2h). Combined, we demonstrated that the T2 distal enhancer regulates endogenous expression of *HHIP* in three types of human lung epithelial cells, BEAS-2B, NHBE and iAT2 cells.

The human unique distal enhancer at 4q31 maintains the topological domain regulating *HHIP* expression

Given that the enhancer is about 60 kb away from the *HHIP* promoter, we performed Hi-C experiments in BEAS-2B cells to elucidate the chromatin interaction dynamics between the 4q31 GWAS locus and the *HHIP* gene body. Publicly available ChIP-seq data in healthy human lung tissues demonstrated the enrichment of H3K27Ac near the distal enhancer T2 region and the *HHIP* promoter (Fig. 3a).[32] More interestingly, corresponding to the H3K27Ac peaks, we detected a robust interaction between the distal enhancer and *HHIP* promoter region in BEAS-2B cells by Hi-C method (Fig. 3a). Such interaction was further confirmed by chromosome conformation capture (3C) assay in BEAS-2B cells (Fig. 3b–d).

Indeed, using publicly available Hi-C data[31] in HHIP-expressing HUVEC cells,[37,38] we found that this identified distal enhancer is perfectly situated between two adjacent chromatin topological domains: one within the 4q31 COPD GWAS locus and the other one spanning the *HHIP* promoter through the gene body (Fig. 3e), suggesting that the identified distal enhancer possibly bridges the interaction of these two interacting regions. To test this hypothesis, we further performed Hi-C experiments in the T2 enhancer KO stable line of BEAS-2B cells. Strikingly, with less than 500bp deletion, T2 enhancer KO cells showed pervasive loss of chromatin interaction near the 4q31 locus and HHIP promoter, as compared to control cells (Fig. 3f). In contrast, nearby adjacent topological domains at 4q remain intact in KO cells (Fig. 3f), suggesting that T2 enhancer is specifically required to maintain the chromatin loops nearby the 4q31 region and *HHIP* gene.

HHIP is induced by TGFβ, independent of the hedgehog pathway in human lung epithelial cells

In addition to its important role in lung development and homeostasis, *HHIP* is also involved in COPD pathogenesis as shown in both human GWAS and mouse models.[7,8] We next set out to determine how HHIP is regulated under COPD-relevant pathological conditions. Given the critical roles of TGFβ in airway remodelling, known to be associated with *HHIP* genotypes in both mouse models and human COPD subjects,[18,39] we asked whether *HHIP* is regulated by TGFβ. Interestingly, *HHIP* expression is induced by TGFβ1 at 6, 12 and 24 h post-treatment in BEAS-2B cells (Fig. 4a). The induction of *HHIP* expression by TGFβ1 was also observed in NHBE cultured at both submerged (Fig. 4b) and air-liquid interface (ALI) conditions (Fig. 4c). It's noteworthy that the recently reported COPD GWAS gene TGFβ2[40,41] also led to a similar induction of *HHIP* in NHBE (SFig. 2a). In contrast, the mouse *Hhip* remains undetectable despite TGFβ1 treatment in primary mouse tracheal epithelial cells, indicative of species-specific induction of HHIP.

HHIP was previously reported as a target of the Hedgehog pathway in multiple cell lines.[42–44] However, treatment with an agonist of Smoothened, SAG, failed to induce expression of *HHIP* and other Hedgehog pathway genes including *GLI1-3* and *PTCH1*, suggesting inactive Hedgehog pathway in NHBE cells (Fig. 4d and Supplementary Fig. S2b–e). Furthermore, *HHIP* is induced by TGFβ1 in the presence of the specific hedgehog inhibitor Vismodegib, the Smoothened antagonist Sonidegib, or the GLI1 inhibitor GANT61 in NHBE (Fig. 4e) and BEAS-2B cells (Supplementary

assays in BEAS-2B cells transfected with various truncated *HHIP* enhancers inserted in front of *HHIP* endogenous promoter (HHIP Pro) in forward (FWD) or reverse (REV) orientations (n = 3 independent transfections) (Statistical analysis: ordinary one-way ANOVA analysis followed by Dunnett comparisons). Conservation analysis of the HHIP promoter (d) and distal enhancer (e) between human and mouse is displayed in green wiggle track according to the UCSC genome browser (hg38) in which the height reflects the size of the conservation score. Single or double horizontal lines above the DNA sequence indicate poor conservation between mice and humans in the region. Measurements of HHIP mRNA levels in BEAS-2B (f) (n = 7 single colonies) or NHBE (g) (n = 3 subjects) cells with CRISPR-edited deletion of the T2 region. Vector-transfected cells were used as wild-type controls (WT) (Statistical analysis: unpaired *t*-test). (h) Measurements of *HHIP* mRNA levels in iPSC-induced alveolar type 2 (iAT2) cells with knockout of the T2 region (n = 3 subjects) (Statistical analysis: ordinary one-way ANOVA analysis followed by Dunnett comparisons). $^{*}P < 0.05$, $^{**}P < 0.01$.

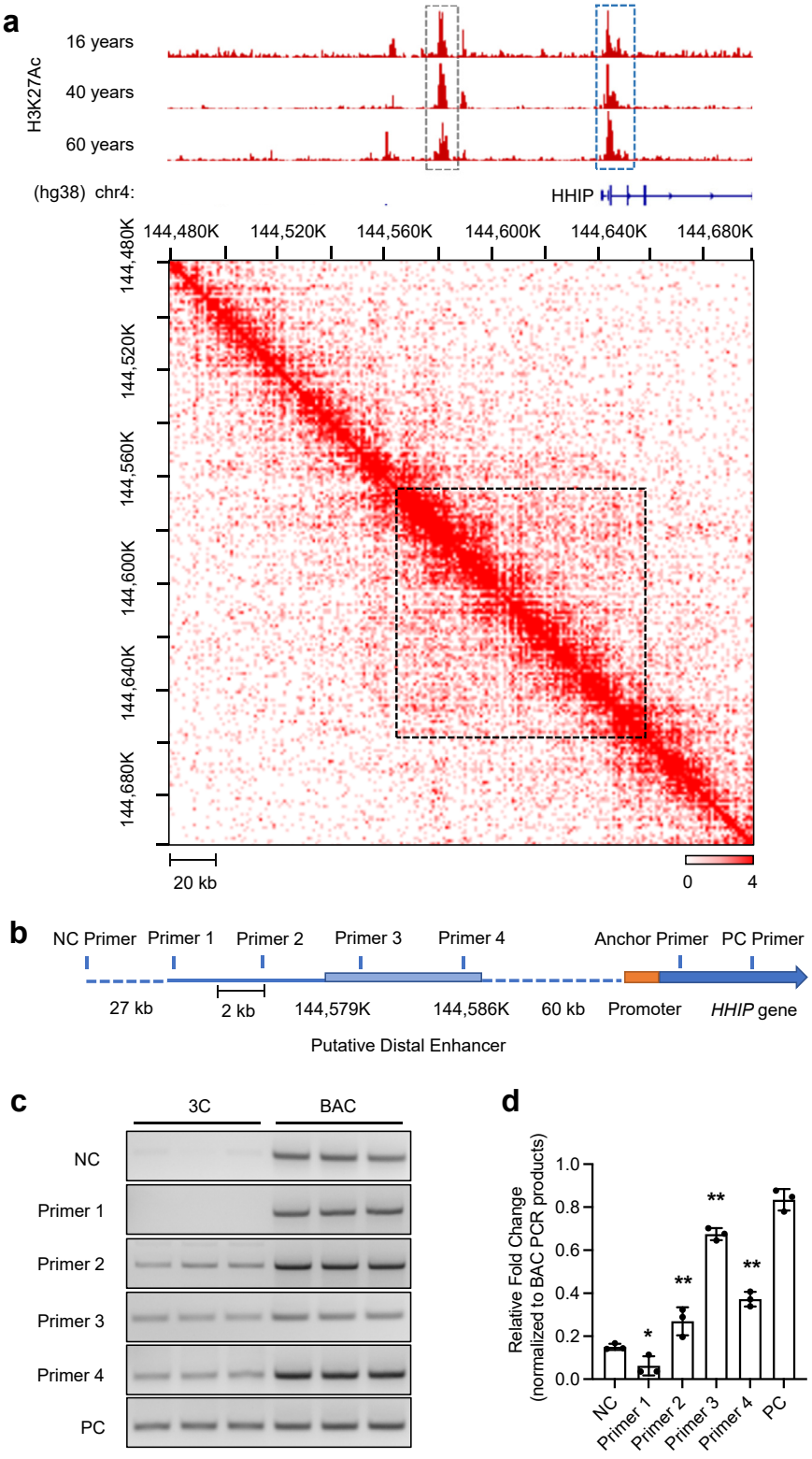

Fig. 3: **Interaction analysis of the *HHIP* distal enhancer and promoter region.** (a) The interaction frequency between the HHIP distal enhancer and promoter is shown by the dotted black frame in the Hi-C matrix from BEAS-2B cells (hg38). The H3K27Ac ChIP-seq peak in lung tissues from human donors at different ages indicates the location of the HHIP distal enhancer and promoter. The dotted grey frame shows the

Fig. S2f), while such induction of HHIP by TGFβ was abolished by TGFβ type I receptor inhibitor SB-431542 (Fig. 4f–h, and Supplementary Fig. S2g) at both RNA and protein levels. These results suggest direct induction of *HHIP* by the activation of the TGFβ signalling pathway, independent of the Hedgehog pathway in human airway epithelial cells.

SMAD3 binds to the *HHIP* distal enhancer upon TGFβ treatment

To investigate whether TGFβ1 induces *HHIP* transcription through distal enhancers that we identified earlier, we performed reporter assays in BEAS-2B cells transfected with T1 to T5 genomic regions in the presence or absence of TGFβ1 treatment. We found that TGFβ1 treatment increased the T2 enhancer activity in both forward and reverse orientations (Fig. 5a), which is accompanied by increased H3K27Ac enrichment (Fig. 5b), indicating activation of *HHIP* distal enhancer by TGFβ1.

TGFβ1 binds to its membrane receptor and leads to phosphorylation and translocation of SMAD3 into nuclei to activate transcription of downstream target genes following the cytoplasmic signalling cascade. Indeed, increased SMAD3-binding was detected near the T2 and T4 enhancer as well as the transcription start site (TSS) of *HHIP* in BEAS-2B cells after TGFβ1 treatment as shown by ChIP-qPCR (Fig. 5c), while stronger SMAD3-binding site is around T2 enhancer region. Furthermore, siRNA targeting SMAD3 led to significantly reduced induction of *HHIP* (Fig. 5d and Supplementary Fig. S3) and reduced enhancer activity of T2 region after TGFβ1 treatment (Fig. 5e).

The T2 enhancer is required for induction of HHIP by TGFβ1 treatment

Additionally, the knockout of T2 enhancer (T2 KO) resulted in weakened SMAD3 binding and reduced H3K27Ac enrichment in the distal enhancers and promoter regions of *HHIP*, and decreased induction of *HHIP* in various clonal BEAS-2B CRISPR lines in response to TGFβ1 (Fig. 6a–d). These findings suggest that deletion of the T2 enhancer caused pervasive epigenetic changes in local chromatin structure, consistent with loss of local chromatin interaction in T2 KO cells (Fig. 3f). Collectively, our findings revealed the T2 enhancer region involved in maintaining both the baseline and induced expression of *HHIP* by TGFβ1.

HHIP knockout promotes EMT in human airway epithelial cells

We have previously reported that after chronic smoke exposure, *Hhip*$^{+/-}$ mice demonstrated increased small airway remodelling,[18] a process usually driven by activation of TGFβ signalling. We next set out to determine whether HHIP regulates the activity of the TGFβ1 pathway. To address this, we generated HHIP knockout BEAS-2B lines by the CRISPR/Cas9 method and assessed the molecular changes induced by TGFβ. We found that the expression of epithelial–mesenchymal transition (EMT) markers such as Cadherin 2 (*CDH2*), Collagen Type IV Alpha 1 Chain (*COL4A1*), and Snail Family Transcriptional Repressor 1 (*SNAI1*) were significantly upregulated in *HHIP* KO cells treated with TGFβ1 for 8 h (Fig. 7a) and 16 h (Fig. 7b) as compared to condition-matched control cells. Furthermore, this was confirmed by western blotting where the protein levels of EMT-related maker genes including N-Cadherin, SNAIL, and SLUG were also increased in *HHIP* KO cells treated with TGFβ1 for 24 and 48 h (Fig. 7c).

Discussion

Our study identified a human unique distal enhancer situated at the boundary of the linkage disequilibrium (LD) block of the 4q31 COPD GWAS locus, regulating expression of *HHIP* gene both at homeostatic condition and upon induction by TGFβ in human lung epithelial cells through examining the chromatin interaction by

H3K27Ac peaks in the distal enhancer region, and the dotted blue frame indicates the peaks in the HHIP promoter region. (b) Relative location of primers used in 3C assays in the human genome according to scales. The orange rectangle indicates the promoter of the *HHIP* gene while the blue rectangle represents the putative distal enhancer (chr4: 144,579K–144,586K, hg38). (c) Results of 3C-PCR in BEAS-2B cells using the primer targeting the *HHIP* promoter as an anchor primer, paired with primers targeting the distal enhancer region, with corresponding BAC as controls (n = 3 PCR reactions). (d) Quantification results of relative band intensity normalised to BAC controls by ImageJ (Statistical analysis: ordinary one-way ANOVA analysis followed by Dunnett comparisons). *$P < 0.05$, **$P < 0.01$. (e) Chromatin Interaction data across the 4q31 COPD GWAS region and *HHIP* gene, based on publicly available Hi-C data in HUVEC cells (hg19) (GSE63525). The dotted black frame indicates the topological domain formed by strong interaction within the 4q31 region, while the dotted blue frame indicates the second topological domain neighbouring the first, extending to the gene body of *HHIP*. The distal enhancer region borders two regions. The H3K27Ac ChIP-seq analysis from HUVEC cells indicates the location of the HHIP distal enhancer and promoter. The dotted grey frame shows the H3K27Ac peaks in the distal enhancer region. (f) Hi-C results from control cells and T2 KO BEAS-2B cells (hg38). The top right corner represents WT results from 2 repeats, and the lower left corner represents KO results from 2 repeats. The dotted black triangle indicates the topological domain spanning the 4q31 GWAS region to the *HHIP* promoter, while the dotted blue triangle indicates the nearby adjacent topological domain spanning the distal enhancer and *HHIP* gene body. 3C: chromosome conformation capture; BAC: bacterial artificial chromosome; PC: positive control; NC: negative control.

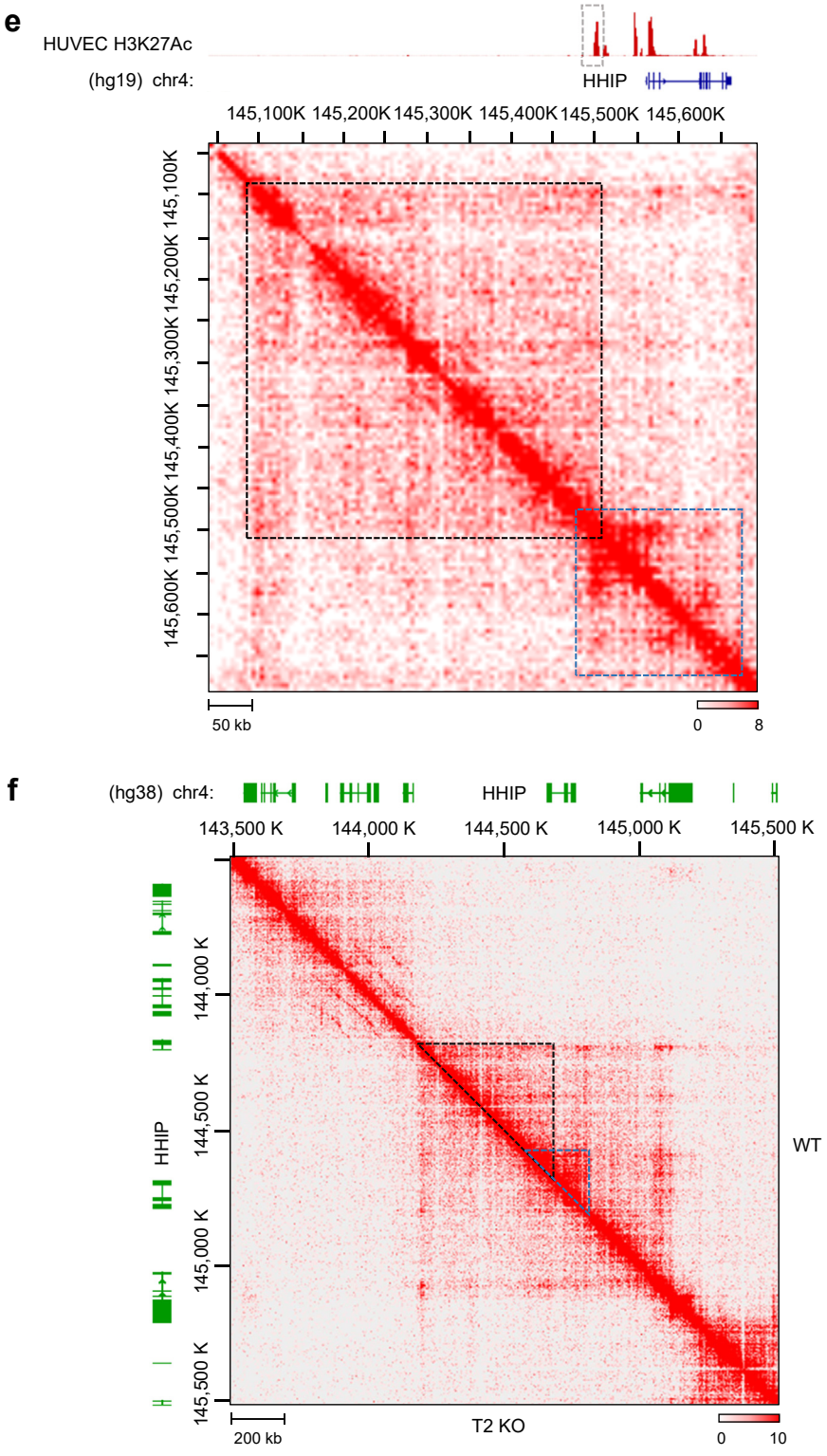

Fig. 3: Continued.

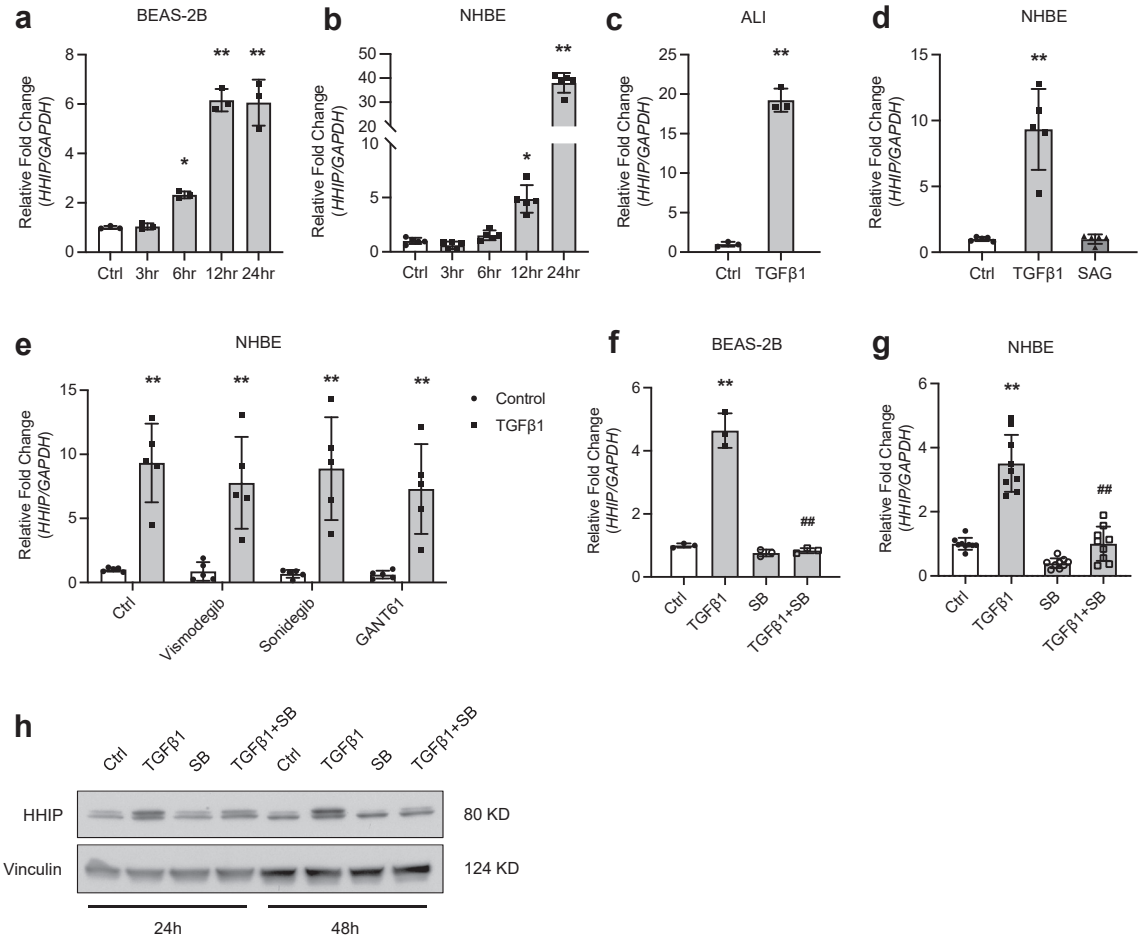

***Fig. 4:* TGFβ induces *HHIP* expression in human bronchial epithelial cells.** Expression of *HHIP* in BEAS-2B cells (n = 3 repeats) (a), primary NHBE cells cultured at submerged condition (n = 5 subjects) (b) or in air-liquid interface (ALI) condition (n = 3 subjects) (c), treated with TGFβ1 (5 ng/mL) for indicated durations. (d) Expression of *HHIP* in primary normal human bronchial epithelial (NHBE) cells treated with TGFβ1 and Hedgehog pathway agonist (n = 5 subjects) or (e) various Hedgehog pathway inhibitors (n = 5 subjects). (f) Expression of *HHIP* in BEAS-2B cells (n = 3 repeats) and (g) primary NHBE cells (n = 3 subjects with 3 repeats) treated with TGFβ1 (5 ng/mL) and/or TGFβ type I receptor inhibitor SB 431542 (SB, 5 μM). (h) Protein levels of HHIP were measured in BEAS-2B cells treated with TGFβ1 (5 ng/mL) and/or TGFβ type I receptor inhibitor SB 431542 (SB, 5 μM) for 24 and 48 h (Statistical analysis for panel a, b, d, f and g: ordinary one-way ANOVA analysis followed by Dunnett comparisons; panel c: unpaired *t*-test; panel e: two-way ANOVA followed by Bonferroni comparisons). $^{*}P < 0.05$, and $^{**}P < 0.01$ comparing to vehicle control group. $^{\#\#}P < 0.01$ comparing to TGFβ1-treated group.

3C and Hi-C as well as epigenetic signatures by ChIP-PCR and snATAC-Seq, combined with genome-editing approaches targeting the T2 enhancer. This poorly conserved enhancer is specifically required to maintain local chromatin interaction, especially around the HHIP promoter and 4q31 region. Furthermore, lung epithelial cells with reduced expression of *HHIP* displayed increased response to TGFβ1 signalling. We not only pinpoint the importance of this regulatory element as an intrinsic enhancer situated at the TADs boundary, but also highlight the biology learned through functional characterization on the distal enhancer within the GWAS locus.

The human genome contains a large number of *cis*-regulatory elements that contribute to cell type-specific gene regulations, resulting in heterogeneous gene expression across various cell types.[45,46] *Cis*-regulatory elements are characterised by highly cell type-specific epigenomic features, such as DNA methylation, histone modifications, as well as conformation of local chromatin, which strongly correlate with cell type-specific gene expression patterns.[45,46] Advanced techniques, such as ChIP-Seq, Hi-C, Hi-ChIP, PLAC-seq, CUT&RUN, and others, have enabled the identification of numerous putative regulatory elements in various tissue/cell types.[47–49] However, subsequent in-depth

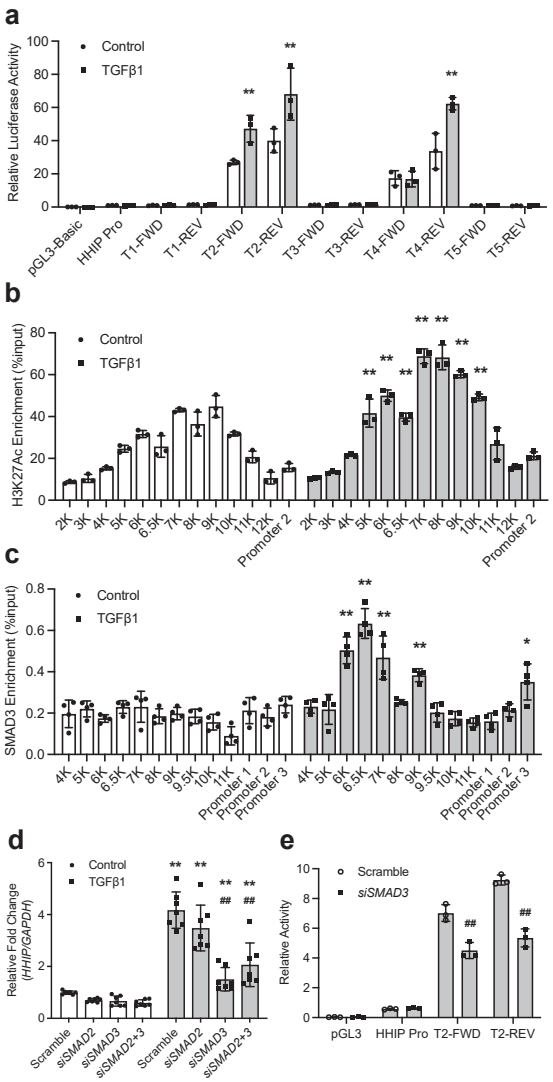

Fig. 5: **TGFβ induces *HHIP* expression in a SMAD3-dependent pathway.** (a) Reporter assay in BEAS-2B cells transfected with truncated enhancers with or without TGFβ1 treatment. H3K27Ac (n = 3 ChIP experiments) (b) and SMAD3 (n = 4 ChIP experiments) (c) enrichment in *HHIP* distal enhancer and promoter region detected by ChIP-qPCR in BEAS-2B cells. (d) Induction of *HHIP* by TGFβ1 was blunted by the knockdown of SMAD3 instead of SMAD2 in BEAS-2B cells (n = 7). (e) Reporter assay in BEAS-2B cells treated with TGFβ1 and transfected with SMAD3 siRNA (n = 3) (Statistical analysis: two-way ANOVA followed by Bonferroni comparisons). $^{*}P < 0.05$, and $^{**}P < 0.01$ comparing to vehicle control group. $^{\#\#}P < 0.01$ compared to the scramble group.

mechanistic studies on these regulatory elements, and possibly using them to interpret the function of GWAS loci associated with complex diseases lag behind. This is particularly important in the post-GWAS era since the majority of genetic variants associated with human complex traits are located in the non-coding regions of the human genome with no clearly assigned genes.[50]

HHIP, a vertebrate-specific negative regulator of the Hedgehog signalling pathway, has attracted increasing attention as one of the most frequently identified genes in GWAS for COPD and lung function. Many components of the Hedgehog signalling pathway have tight regulation in a wide range of processes, such as during the development of limbs and regulation of left-right asymmetry in embryonic development.[6,51,52] Sonic hedgehog (SHH), an important agonist of the Hedgehog signalling pathway controlling embryonic limb development, is strictly regulated by a distal enhancer (~1 Mb away).[53] The minimal 17 bp enhancer region is highly conserved in all examined limbed vertebrates but deleted in snakes. In contrast, the T2 enhancer for *HHIP* described herein lacks conservation between humans and mice, possibly indicating different transcriptional regulation of *HHIP* in human cells.

Our interesting finding that the deletion of the T2 enhancer (~500 bp) in BEAS-2B cells led to a reduction of chromatin interaction frequency (Fig. 3f) and loss of nearby epigenetic markers (Fig. 6c) highlights the importance of this human unique T2 enhancer. In addition to cellular models, recent functional studies on the boundary elements of topologically associated domains (TADs) in mouse models also indicate significant changes in mouse model phenotype, gene expression and chromatin interactions when boundary elements were depleted.[54] However, such pervasive changes caused by the depletion of each individual boundary element are likely context-specific.

Given its genomic location, this human-specific *HHIP* distal enhancer may be located at a 'transition zone' that was reported previously to be moderately insulated and may exhibit cell-to-cell variation of loop extrusion blocking and readthrough regulation mechanism.[55,56] Through partition of the topological domains, T2 enhancer may potentially facilitate the regulation of *HHIP* expression by genetic variants within the 4q31 GWAS locus in a context-specific manner, possibly enabling more complex and fine regulation of human *HHIP*, the important GWAS gene associated with multiple complex traits including height, lung function and COPD.[57–59]

The distal enhancer region is located with the linkage disequilibrium (LD) block of the 4q31 COPD GWAS locus. However, no GWAS variants are directly located inside the enhancer T2 region. This raised a couple of possibilities: 1) These enhancers are essential for HHIP transcriptional regulation. Given the importance of HHIP during embryonic development, any genetic variants that are directly located inside the enhancer may impact its activity and are unable to survive the evolutionary pressure due to lethal effects. This is consistent with the well-accepted notion that the function and positions of such boundary elements are subject to evolutionary constraint,[60–62] which explains the overall depletion of structural variants at TAD

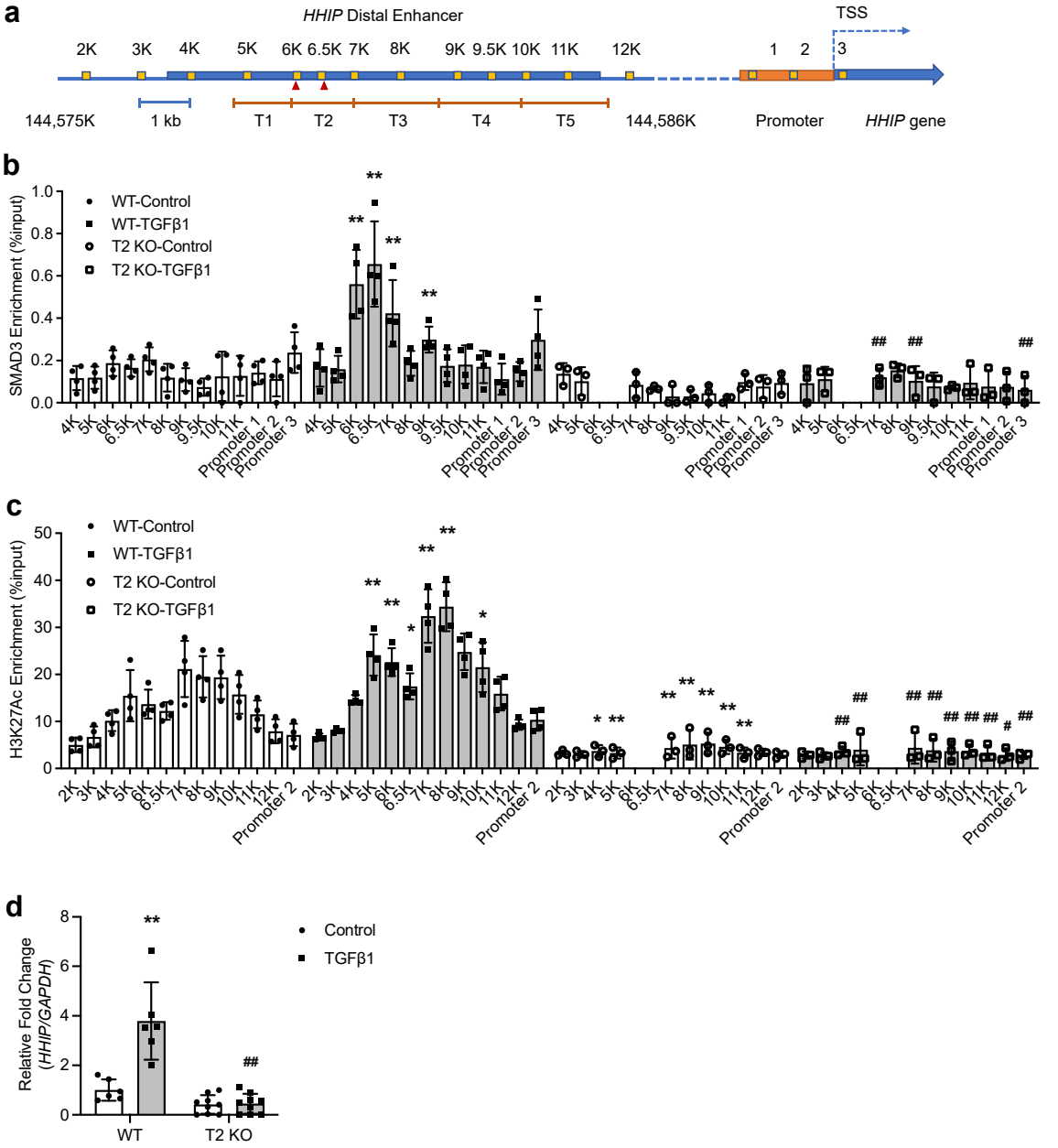

***Fig. 6*: Distal enhancer region knockout reduces *HHIP* expression level.** (a) A diagram indicating the relative location of ChIP-qPCR primers and CRISPR/Cas9 gRNAs (red solid triangles). SMAD3 (b) or H3K27Ac enrichment (c) detected by ChIP-qPCR with or without TGFβ1 treatment in T2 region knockout (T2 KO) BEAS-2B single colonies (n = 3–4 single colonies). (d) *HHIP* mRNA levels were measured in T2 KO BEAS-2B single colonies with or without TGFβ1 treatment (n = 6–9 single colonies). (Statistical analysis for panel b and c: two-way ANOVA followed by multiple unpaired t-tests; panel d: ordinary one-way ANOVA analysis followed by Dunnett comparisons). $^{*}P < 0.05$, and $^{**}P < 0.01$ comparing to WT vehicle control group; $^{\#}P < 0.05$, and $^{\#\#}P < 0.01$ comparing to WT TGF-β1 treated group.

boundaries. 2) COPD GWAS variants located in the flanking sequence of the distal enhancer, may also modulate the activity of the distal enhancer as demonstrated recently.[63] These possibilities will be carefully evaluated in our future experiments.

HHIP was known to be induced by the Hedgehog pathway to constrain its overactivation, forming the negative feedback loop in mouse mesenchymal cells.[6] Similarly, in human airway epithelial cells, TGFβ induced expression of *HHIP* by binding of SMAD3 to

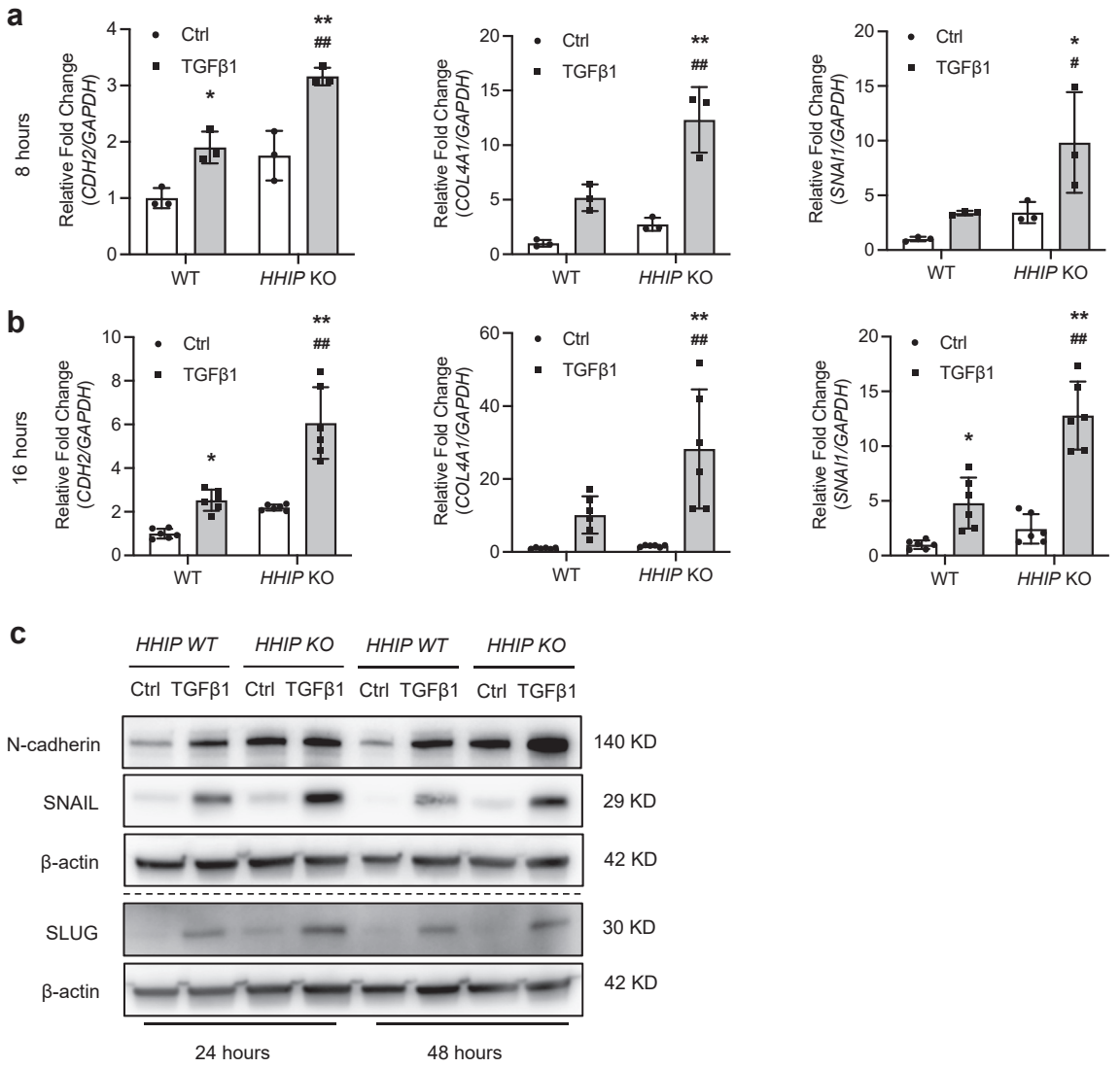

***Fig. 7*: *HHIP* represses EMT induced by TGFβ in human airway epithelial cells.** Expression of epithelial–mesenchymal transition (EMT) marker genes, *CDH2*, *COL4A1*, and *SNAI1* was measured in WT or *HHIP* KO BEAS-2B cells with or without TGFβ1 treatment for 8 h (n = 3) (a) or 16 h (n = 5) (b). (c) Representative results showing expression of epithelial–mesenchymal transition (EMT) marker genes, N-cadherin, SNAIL, and SLUG in WT or *HHIP* KO BEAS-2B cells with or without TGFβ1 treatment for 24 and 48 h (Statistical analysis: two-way ANOVA followed by Bonferroni comparisons). $^{*}P < 0.05$, and $^{**}P < 0.01$ with/without TGFβ1 treatment; $^{\#}P < 0.05$, and $^{\#\#}P < 0.01$ with/without *HHIP* KO.

the distal enhancer, independent of the Hedgehog pathway. Furthermore, given increased expression of EMT marker genes in HHIP knockout BEAS-2B cells, HHIP may serve to shape cell autonomous epithelial-specific response to TGFβ. However, *Hhip* was also reported to activate the Tgfb1-Smad2/3 cascade and promote mouse endothelial to mesenchymal transition,[64] indicative of a cell type-specific regulation between TGFβ and *HHIP*. Therefore, we need to be cautious and mindful when interpreting the context-specific interplay between HHIP and the TGFβ pathway.

The TGFβ pathway is a key mediator of airway remodelling in COPD.[15] Additionally, increased TGFβ1 protein levels were detected in the airway epithelium of patients with COPD.[15,65] Furthermore, a subgroup of airway epithelial colonies generated from patients with COPD constitutively express genes enriched in the TGFβ2 pathway that may drive pro-fibrotic effects, contributing to small airway remodelling in COPD,[40] indicating the importance of TGFβ signalling in COPD. Future investigations are required on how HHIP interacts with TGFβ signalling under pathological

conditions to shape the development of COPD. Furthermore, there are additional growth factors important for COPD pathogenesis. Whether and how HHIP is also regulated by other COPD-relevant growth factors requires systematic investigations in the future.

The limitations of our study include: 1) The sample size of COPD lungs used in the snATAC-Seq experiments is quite small. Therefore, any comparisons between COPD and healthy control lungs need to be confirmed in a larger sample size in follow-up studies given the heterogeneity of COPD. 2) The complex interplay between HHIP and TGFβ signalling needs to be carefully evaluated further in the context of COPD development in future studies. 3) The direct impacts of the enhancer on COPD development require further investigation, possibly in other mammals such as non-human primates that share the enhancer sequence with humans. Nonetheless, our current study reports transcriptional regulation of *HHIP* by a human unique distal enhancer located at the COPD 4q31 GWAS locus. This regulation occurs both at baseline and after TGFβ1 induction in human bronchial epithelial cells. Conversely, HHIP represses TGFβ-induced EMT, suggesting complex signalling interaction between HHIP and TGFβ. Given the complex dynamic of cell quiescence, proliferation and differentiation transition during homeostasis and lung repair/regeneration, further investigations into the context-specific regulation of HHIP by various transcription factors and other epigenetic modifications under pathologic conditions are necessary to gain deeper mechanistic insights. Ultimately, this knowledge could help pinpoint potential treatment strategies for COPD.

Contributors

X. Z and F. G designed and supervised the overall study. F. G and L. Z performed most of the experiments and results analysis. Y. Y performed Hi-C experiments. H. I, W. W, Y. Zhou, W. J. A, and Y. Y ran RT-qPCR and Western blot experiments. L. G, S. T and W. C performed the ATAC-seq and scRNA-seq analysis. R. B. W and A. W designed and performed experiments in iAT2 cells. T. Lao helps with TGFβ stimulation experiments. S. M and M. H analysed the Hi-C analysis. Y. Zhang and H. M designed and performed the ALI experiments. F. G and B. P performed the reporter assays. T. Liu generated an *HHIP* knockout BEAS-2B cell line. B. R and T. T generated the snATAC-seq libraries. F. G and X. Z verified the data and wrote the manuscript which all authors reviewed and approved.

Data sharing statement

All raw data in the study will be made available from the lead contact upon any reasonable request.

Declaration of interests

All authors have read and confirmed the manuscript and accepted the responsibility to submit it for publication. No potential conflicts of interest for all authors listed in the manuscript.

Acknowledgements

This work was supported by the National Heart, Lung, and Blood Institute of the National Institutes of Health grants R01HL127200, R01HL148667 and R01HL162783 to X. Z, National Institute of Arthritis and Musculoskeletal and Skin Diseases (United States) grant R21AR080778 to H. M, IK2BX003841 from the Department of Veterans Affairs to B.W.R and a generous gift from the Ann M. Duffer Family Foundation. We acknowledge the ENCODE Consortium and the ENCODE production laboratory generating the H3K27Ac ChIP-seq datasets.

Appendix A. Supplementary data

Supplementary data related to this article can be found at https://doi.org/10.1016/j.ebiom.2024.105026.

References

1 Boueiz A, Lutz SM, Cho MH, et al. Genome-wide association study of the genetic determinants of emphysema distribution. *Am J Respir Crit Care Med*. 2017;195(6):757–771.
2 Morrow JD, Zhou X, Lao T, et al. Functional interactors of three genome-wide association study genes are differentially expressed in severe chronic obstructive pulmonary disease lung tissue. *Sci Rep*. 2017;7:44232.
3 Ragland MF, Benway CJ, Lutz SM, et al. Genetic advances in chronic obstructive pulmonary disease. Insights from COPDGene. *Am J Respir Crit Care Med*. 2019;200(6):677–690.
4 Shrine N, Izquierdo AG, Chen J, et al. Multi-ancestry genome-wide association analyses improve resolution of genes and pathways influencing lung function and chronic obstructive pulmonary disease risk. *Nat Genet*. 2023;55(3):410–422.
5 Chuang PT, McMahon AP. Vertebrate Hedgehog signalling modulated by induction of a Hedgehog-binding protein. *Nature*. 1999;397(6720):617–621.
6 Chuang PT, Kawcak T, McMahon AP. Feedback control of mammalian Hedgehog signaling by the Hedgehog-binding protein, Hip1, modulates Fgf signaling during branching morphogenesis of the lung. *Genes Dev*. 2003;17(3):342–347.
7 Lao T, Glass K, Qiu W, et al. Haploinsufficiency of Hedgehog interacting protein causes increased emphysema induced by cigarette smoke through network rewiring. *Genome Med*. 2015;7(1):12.
8 Lao T, Jiang Z, Yun J, et al. Hhip haploinsufficiency sensitizes mice to age-related emphysema. *Proc Natl Acad Sci U S A*. 2016;113(32):E4681–E4687.
9 Yun JH, Lee C, Liu T, et al. Hedgehog interacting protein-expressing lung fibroblasts suppress lymphocytic inflammation in mice. *JCI Insight*. 2021;6(17):e144575.
10 Tauriello DVF, Sancho E, Batlle E. Overcoming TGFbeta-mediated immune evasion in cancer. *Nat Rev Cancer*. 2022;22(1):25–44.
11 Gilbert RWD, Vickaryous MK, Viloria-Petit AM. Signalling by transforming growth factor beta isoforms in wound healing and tissue regeneration. *J Dev Biol*. 2016;4(2):21.
12 Batlle E, Massague J. Transforming growth factor-beta signaling in immunity and cancer. *Immunity*. 2019;50(4):924–940.
13 Shen HJ, Sun YH, Zhang SJ, et al. Cigarette smoke-induced alveolar epithelial-mesenchymal transition is mediated by Rac1 activation. *Biochim Biophys Acta*. 2014;1840(6):1838–1849.
14 Wang Z, Fang K, Wang G, et al. Protective effect of amygdalin on epithelial-mesenchymal transformation in experimental chronic obstructive pulmonary disease mice. *Phytother Res*. 2019;33(3):808–817.
15 Takizawa H, Tanaka M, Takami K, et al. Increased expression of transforming growth factor-beta1 in small airway epithelium from tobacco smokers and patients with chronic obstructive pulmonary disease (COPD). *Am J Respir Crit Care Med*. 2001;163(6):1476–1483.
16 Liu G, Philp AM, Corte T, et al. Therapeutic targets in lung tissue remodelling and fibrosis. *Pharmacol Ther*. 2021;225:107839.
17 Yang YC, Zhang N, Van Crombruggen K, Hu GH, Hong SL, Bachert C. Transforming growth factor-beta1 in inflammatory airway disease: a key for understanding inflammation and remodeling. *Allergy*. 2012;67(10):1193–1202.
18 Li Y, Zhang L, Polverino F, et al. Hedgehog interacting protein (HHIP) represses airway remodeling and metabolic reprogramming in COPD-derived airway smooth muscle cells. *Sci Rep*. 2021;11(1):9074.
19 Hao Y, Hao S, Andersen-Nissen E, et al. Integrated analysis of multimodal single-cell data. *Cell*. 2021;184(13):3573–3587.e29.
20 Stuart T, Srivastava A, Madad S, Lareau CA, Satija R. Single-cell chromatin state analysis with Signac. *Nat Methods*. 2021;18(11):1333–1341.

21 Zhang Y, Liu T, Meyer CA, et al. Model-based analysis of ChIP-seq (MACS). *Genome Biol*. 2008;9(9):R137.
22 Travaglini KJ, Nabhan AN, Penland L, et al. A molecular cell atlas of the human lung from single-cell RNA sequencing. *Nature*. 2020;587(7835):619–625.
23 Levardon H, Yonker LM, Hurley BP, Mou H. Expansion of airway basal cells and generation of polarized epithelium. *Bio Protoc*. 2018;8(11):e2877.
24 Jiang Z, Lao T, Qiu W, et al. A chronic obstructive pulmonary disease susceptibility gene, FAM13A, regulates protein stability of beta-catenin. *Am J Respir Crit Care Med*. 2016;194(2):185–197.
25 Zhou X, Baron RM, Hardin M, et al. Identification of a chronic obstructive pulmonary disease genetic determinant that regulates HHIP. *Hum Mol Genet*. 2012;21(6):1325–1335.
26 Blanchette M, Kent WJ, Riemer C, et al. Aligning multiple genomic sequences with the threaded blockset aligner. *Genome Res*. 2004;14(4):708–715.
27 Werder RB, Liu T, Abo KM, et al. CRISPR interference interrogation of COPD GWAS genes reveals the functional significance of desmoplakin in iPSC-derived alveolar epithelial cells. *Sci Adv*. 2022;8(28):eabo6566.
28 Zhang H, Song L, Wang X, et al. Fast alignment and preprocessing of chromatin profiles with Chromap. *Nat Commun*. 2021;12(1):6566.
29 Durand NC, Shamim MS, Machol I, et al. Juicer provides a one-click system for analyzing loop-resolution Hi-C experiments. *Cell Syst*. 2016;3(1):95–98.
30 Robinson JT, Turner D, Durand NC, Thorvaldsdottir H, Mesirov JP, Aiden EL. Juicebox.js provides a cloud-based visualization system for Hi-C data. *Cell Syst*. 2018;6(2):256–258 e1.
31 Rao SS, Huntley MH, Durand NC, et al. A 3D map of the human genome at kilobase resolution reveals principles of chromatin looping. *Cell*. 2014;159(7):1665–1680.
32 Consortium EP. An integrated encyclopedia of DNA elements in the human genome. *Nature*. 2012;489(7414):57–74.
33 Adams TS, Schupp JC, Poli S, et al. Single-cell RNA-seq reveals ectopic and aberrant lung-resident cell populations in idiopathic pulmonary fibrosis. *Sci Adv*. 2020;6(28):eaba1983.
34 Tabula Muris C. A single-cell transcriptomic atlas characterizes ageing tissues in the mouse. *Nature*. 2020;583(7817):590–595.
35 Benway CJ, Liu J, Guo F, et al. Chromatin landscapes of human lung cells predict potentially functional chronic obstructive pulmonary disease genome-wide association study variants. *Am J Respir Cell Mol Biol*. 2021;65(1):92–102.
36 Wang A, Chiou J, Poirion OB, et al. Single-cell multiomic profiling of human lungs reveals cell-type-specific and age-dynamic control of SARS-CoV2 host genes. *Elife*. 2020;9:e62522.
37 Sekiguchi H, Ii M, Jujo K, et al. Estradiol triggers sonic-hedgehog-induced angiogenesis during peripheral nerve regeneration by downregulating hedgehog-interacting protein. *Lab Invest*. 2012;92(4):532–542.
38 Niu C, Chen Z, Kim KT, et al. Metformin alleviates hyperglycemia-induced endothelial impairment by downregulating autophagy via the Hedgehog pathway. *Autophagy*. 2019;15(5):843–870.
39 van der Plaat DA, de Jong K, Lahousse L, et al. The well-known gene HHIP and novel gene MECR are implicated in small airway obstruction. *Am J Respir Crit Care Med*. 2016;194(10):1299–1302.
40 Rao W, Wang S, Duleba M, et al. Regenerative metaplastic clones in COPD lung drive inflammation and fibrosis. *Cell*. 2020;181(4):848–864.e18.
41 Parker MM, Hao Y, Guo F, et al. Identification of an emphysema-associated genetic variant near TGFB2 with regulatory effects in lung fibroblasts. *Elife*. 2019;8:e42720.
42 Lahmar Z, Ahmed E, Fort A, Vachier I, Bourdin A, Bergougnoux A. Hedgehog pathway and its inhibitors in chronic obstructive pulmonary disease (COPD). *Pharmacol Ther*. 2022;240:108295.
43 Sigafoos AN, Paradise BD, Fernandez-Zapico ME. Hedgehog/GLI signaling pathway: transduction, regulation, and implications for disease. *Cancers*. 2021;13(14):3410.
44 Choi SS, Omenetti A, Witek RP, et al. Hedgehog pathway activation and epithelial-to-mesenchymal transitions during myofibroblastic transformation of rat hepatic cells in culture and cirrhosis. *Am J Physiol Gastrointest Liver Physiol*. 2009;297(6):G1093–G1106.
45 Heintzman ND, Hon GC, Hawkins RD, et al. Histone modifications at human enhancers reflect global cell-type-specific gene expression. *Nature*. 2009;459(7243):108–112.
46 Janssens DH, Wu SJ, Sarthy JF, et al. Automated in situ chromatin profiling efficiently resolves cell types and gene regulatory programs. *Epigenet Chromatin*. 2018;11(1):74.
47 Whyte WA, Orlando DA, Hnisz D, et al. Master transcription factors and mediator establish super-enhancers at key cell identity genes. *Cell*. 2013;153(2):307–319.
48 Wilhelm T. Phenotype prediction based on genome-wide DNA methylation data. *BMC Bioinf*. 2014;15:193.
49 Tobias IC, Abatti LE, Moorthy SD, et al. Transcriptional enhancers: from prediction to functional assessment on a genome-wide scale. *Genome*. 2021;64(4):426–448.
50 Tam V, Patel N, Turcotte M, Bosse Y, Pare G, Meyre D. Benefits and limitations of genome-wide association studies. *Nat Rev Genet*. 2019;20(8):467–484.
51 Marigo V, Scott MP, Johnson RL, Goodrich LV, Tabin CJ. Conservation in hedgehog signaling: induction of a chicken patched homolog by Sonic hedgehog in the developing limb. *Development*. 1996;122(4):1225–1233.
52 van den Brink GR. Hedgehog signaling in development and homeostasis of the gastrointestinal tract. *Physiol Rev*. 2007;87(4):1343–1375.
53 Kvon EZ, Kamneva OK, Melo US, et al. Progressive loss of function in a limb enhancer during snake evolution. *Cell*. 2016;167(3):633–642.e11.
54 Rajderkar S, Barozzi I, Zhu Y, et al. Topologically associating domain boundaries are required for normal genome function. *Commun Biol*. 2023;6(1):435.
55 Chang LH, Ghosh S, Papale A, et al. Multi-feature clustering of CTCF binding creates robustness for loop extrusion blocking and Topologically Associating Domain boundaries. *Nat Commun*. 2023;14(1):5615.
56 Chang LH, Ghosh S, Noordermeer D. TADs and their borders: free movement or building a wall? *J Mol Biol*. 2020;432(3):643–652.
57 van der Plaat DA, de Jong K, Lahousse L, et al. Genome-wide association study on the FEV(1)/FVC ratio in never-smokers identifies HHIP and FAM13A. *J Allergy Clin Immunol*. 2017;139(2):533–540.
58 Zhang Z, Wang J, Zheng Z, et al. Genetic variants in the hedgehog interacting protein gene are associated with the FEV1/FVC ratio in southern han Chinese subjects with chronic obstructive pulmonary disease. *BioMed Res Int*. 2017;2017:2756726.
59 Ortega-Martinez A, Perez-Rubio G, Ramirez-Venegas A, et al. Participation of HHIP gene variants in COPD susceptibility, lung function, and serum and sputum protein levels in women exposed to biomass-burning smoke. *Diagnostics*. 2020;10(10):734.
60 Vietri Rudan M, Hadjur S. Genetic tailors: CTCF and cohesin shape the genome during evolution. *Trends Genet*. 2015;31(11):651–660.
61 Krefting J, Andrade-Navarro MA, Ibn-Salem J. Evolutionary stability of topologically associating domains is associated with conserved gene regulation. *BMC Biol*. 2018;16(1):87.
62 Fudenberg G, Pollard KS. Chromatin features constrain structural variation across evolutionary timescales. *Proc Natl Acad Sci U S A*. 2019;116(6):2175–2180.
63 Horton CA, Alexandari AM, Hayes MGB, et al. Short tandem repeats bind transcription factors to tune eukaryotic gene expression. *Science*. 2023;381(6664):eadd1250.
64 Zhao XP, Chang SY, Liao MC, et al. Hedgehog interacting protein promotes fibrosis and apoptosis in glomerular endothelial cells in murine diabetes. *Sci Rep*. 2018;8(1):5958.
65 Gohy ST, Detry BR, Lecocq M, et al. Polymeric immunoglobulin receptor down-regulation in chronic obstructive pulmonary disease. Persistence in the cultured epithelium and role of transforming growth factor-beta. *Am J Respir Crit Care Med*. 2014;190(5):509–521.